



## SCATTERING FROM PARABOLIC CYLINDRICAL REFLECTOR ANTENNA USING PHYSICAL OPTICS

Fadıl KUYUCUOĞLU<sup>1\*</sup>

<sup>1</sup>Manisa Celal Bayar University, Faculty of Engineering, Department of Electrical-Electronics Engineering, 45140, Manisa, Türkiye

**Abstract:** In this study, numerical analysis of scattering from a dielectric-coated metallic reflector is presented. The reflector has a parabolic cross-sectional cylindrical geometry. Radiation patterns and aperture efficiency parameters are analyzed using physical optics. A complex source point located at the focal point of the parabolic reflector is used as the source of radiation. The dielectric-coated metallic reflector is considered as an antenna, and an impedance boundary is utilized. The effects of coating on radiation patterns are analyzed in terms of dielectric thickness and dielectric permittivity. Numerical results are presented for various parameters, including dielectric permittivity, dielectric layer thickness, complex source point width, and focal distance.

**Keywords:** Scattering, Physical optics, Impenetrable sheet, Cylindrical parabolic reflector

\*Corresponding author: Manisa Celal Bayar University, Faculty of Engineering, Department of Electrical-Electronics Engineering, 45140, Manisa, Türkiye

E mail: fadil.kuyucuoglu@cbu.edu.tr (F. KUYUCUOĞLU)

Fadıl KUYUCUOĞLU  <https://orcid.org/0000-0002-0134-0491>

Received: August 07, 2023

Accepted: September 29, 2023

Published: October 15, 2023

Cite as: Kuyucuoglu F. 2023. Scattering from parabolic cylindrical reflector antenna using physical optics. BSJ Eng Sci, 6(4): 550-556.

### 1. Introduction

In antenna design, reflector antennas have been widely used in applications such as satellite communications, radio astronomy, remote sensing, and radar (Rahmat-Samii and Haupt, 2015; Lu and Qu, 2023). Among reflector antennas, the parabolic reflector is the most preferred type due to its improved overall radiation characteristics (Balanis, 2016). Parabolic reflectors exhibit lower sidelobes and higher beam efficiencies compared to other reflectors (Wu et al., 2016).

However, in parabolic reflector antennas with fixed geometry, the performance depends on the feeder located along the focus axis of the reflector. Adjusting the focal length is crucial for achieving higher gain. Unfortunately, locating the feeder causes aperture-blocking effects, negatively affecting the radiation patterns and gain of the antenna (Quadrat and Shafai, 2012). To increase the gain of the antenna, a common and simple approach is to add a perfect electric conductor (PEC) on the reflector surface (Ge et al., 2018; Chang et al., 2021; Wu et al., 2021). Additionally, a high focal-to-diameter ( $f/D$ ) ratio enables a high aperture efficiency for the reflector antenna (Galuscak et al., 2018; Granet et al., 2005; Wang et al., 2020).

It is worth mentioning that the characteristics of reflector surfaces also significantly impact the radiation properties of antennas. Impedance surfaces find considerable applications in the modeling of reflector antennas in optics and electromagnetics studies (Bhattacharyya, 1995). Many studies have presented the scattering from impedance surfaces (Kuyucuoglu et al., 2014; Maliuzhinets, 1959; Tiberio et al., 1985; Volakis, 1986;

Umul, 2006; Umul, 2007; Bie et al., 2023).

In this study, scattering from a dielectric-coated perfectly electric conductor (PEC) cylindrical parabolic reflector antenna is analyzed. The complex source point is used as the feed and is located at the focus of the reflector. Impedance boundary conditions are utilized, and the physical optics (PO) method is used to obtain the radiation pattern, as explained in (Umul, 2008). The impedance of the surface is evaluated using the expressions given in (Bleszynski et al., 1993) as impenetrable thin layer systems.

By using the PO method, the surface integrals are evaluated asymptotically. The performance of the reflector is analyzed for several dielectric thickness and focal length parameters. Throughout the paper, a time factor  $\exp(-j\omega t)$  is used and omitted.

### 2. Materials and Methods

The cylindrical parabolic reflector antenna shown in Figure 1 is fed by a complex source point (CSP), with the feed located precisely at the focus ( $f$ ) of the parabolic reflector. The aperture of the reflector is represented by the symbol  $D$ . The antenna is constructed using infinitely thin PEC (Perfect Electric Conductor) material, and this PEC material is coated with a dielectric material. The antenna lies on the  $x$ - $y$  plane and extends infinitely in the  $z$ -axis direction. The cross-sectional shape of the reflector is parabolic, and the feed is precisely placed at the focus of this parabolic geometry.



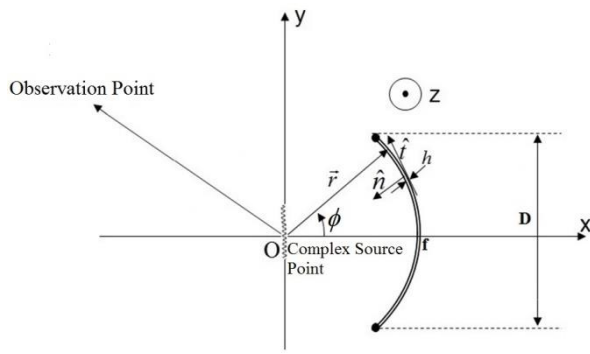


Figure 1. Problem geometry

In the case of E-polarization, electric and magnetic field components are taken as  $E_z$ ,  $H_x$  and  $H_y$  respectively. If we choose  $E_z$  as the basic component and denote it, complex source point can be expressed as (equation 1):

$$U^{in}(\vec{r}) = H_0^{(1)}(k_0|\vec{r} - (\vec{r}_0 + i\vec{b})|) \quad (1)$$

where  $H_0^{(1)}$  is the Hankel function of the first kind,  $\vec{r}$  is the position vector,  $\vec{r}_0$  is the real source position vector of the CSP,  $b$  is the aperture width of the CSP and  $k_0$  is the wavenumber in free space.

In order to model the surface of the reflector, impenetrable boundary condition is utilized. We can write the impedance of the sheet face in (equation 2) as described in (Bleszynski et al., 1993) for nonmagnetic materials.

$$Z = -i \frac{Z_0}{\sqrt{\epsilon_r}} \tan(\sqrt{\epsilon_r} k_0 d) \quad (2)$$

In equation (2), the variable  $d$  is defined as the thickness of the dielectric coating, and  $\epsilon_r$  is the relative dielectric constant of the material.

After defining the feed and antenna impedance, the next step is to write the sum of the scattered field and the incident field using the physical optics as in Equation (3). The integral for the electrical line source and impedance surface in this equation is described in detail in (Umul, 2008). However, for the current study, this theory is being modified to account for a complex source point feed and several coatings on the PEC reflector.

The physical optics method takes into consideration the effects of the complex source point feed and the multiple dielectric coatings on the reflector's surface. These modifications allow for a more accurate representation of the radiation pattern and characteristics of the reflector antenna. The scattering and radiation behavior are now computed considering the presence of the complex source point and the interactions with the impedance surface of the dielectric-coated reflector.

By incorporating these modifications into the theoretical framework, the study aims to obtain a comprehensive understanding of the antenna's performance when fed by a complex source point and coated with various dielectric materials. The detailed analysis presented in (Umul, 2008) for the electrical line source and impedance

surface is extended and adapted to suit the current scenario with a complex source point and multiple coatings on the PEC reflector.

$$E_{tot} = \frac{e^{jkr}}{\sqrt{kr}} \left( e^{j\theta \cos(\phi)} + \frac{ke^{j\pi/4}}{\sqrt{2\pi}} \int_{-\theta}^{\theta} \left[ \frac{\sin(\alpha) - (Z_0/Z)}{\sin(\alpha) + (Z_0/Z)} \right] \sin(\alpha) \left[ \frac{e^{jkr'(\phi)} e^{j\theta \cos(\phi)}}{\sqrt{k}} e^{-jkr'(\phi) \cos(\phi - \phi')} \right] \frac{\sqrt{f}}{\cos^2(\phi'/2)} d\phi' \right) \quad (3)$$

In equation (3), total field expression is given where

$\alpha = \left(\frac{\pi}{2}\right) - \left(\frac{\theta'}{2}\right)$ ,  $r'(\phi') = f/\cos^2(\frac{\theta'}{2})$ ,  $f$  is the focal length of reflector,  $Z_0$  is the free space impedance,  $\theta_0$  is the angle of the aperture of the reflector. CSP is located at the focus where we can write  $\vec{r}_0 = 0$ .

After obtaining total fields, forward directivity ( $D_0$ ) is calculated taking the integral of total field given in Equation (3). Besides, aperture efficiency can be calculated as in Equation (4) easily.

$$\epsilon_{eff} = \frac{D_0}{2\pi D} \quad (4)$$

In the following section, antenna performance is presented with several coating thicknesses, CSP width, focal distances.

### 3. Results and Discussion

In the analysis, an impenetrable, impedance surface, parabolic reflector antenna is studied under E-polarized CSP (Complex Source Point) illumination. All metric parameters are given in terms of free space wavelength ( $\lambda_0$ ).

Initially, the total radiated field is calculated for a PEC reflector with dielectric coatings with various thicknesses. The variation of the total field is presented in dB scale in Figure 2. For this calculation, the width of the CSP ( $kb$ ) is chosen as 3 and the aperture width of the antenna ( $D$ ) is selected as 10. The focus of the parabolic reflector is set at 5.

Several coatings are considered for the reflector antenna. Specifically, tantalum oxide with  $\epsilon_r=20$  and silicon with  $\epsilon_r=11.7$  are investigated. This study examines the impact of different dielectric thicknesses ( $d$ ) on the levels of backside radiation.

As shown in Figure 2, for the tantalum oxide coating ( $\epsilon_r=20$ ) with  $\lambda_0/200$  thickness case, minimum backside radiation occurs. However, as the magnitude of the impedance of the dielectric coating increases, higher levels of backside radiation are observed between  $120^\circ$  and  $180^\circ$ . Front side radiation levels are nearly the same for all the cases under investigation. In order to prove the correctness of the backside radiation of PO, method of analytical regularization (MAR) results are used for comparison purposes. It can be seen that, front side radiations are nearly same for PO and MAR as expected but small deviations are observed at the backside region. The results of the analysis highlight the importance of the dielectric coating and its thickness in shaping the radiation pattern of the reflector antenna. Different

dielectric materials with distinct permittivity values yield varying levels of backside radiation, while the front side radiation remains relatively consistent. These findings

contribute to a deeper understanding of the antenna's performance and may guide the selection of suitable dielectric coatings for desired radiation characteristics.

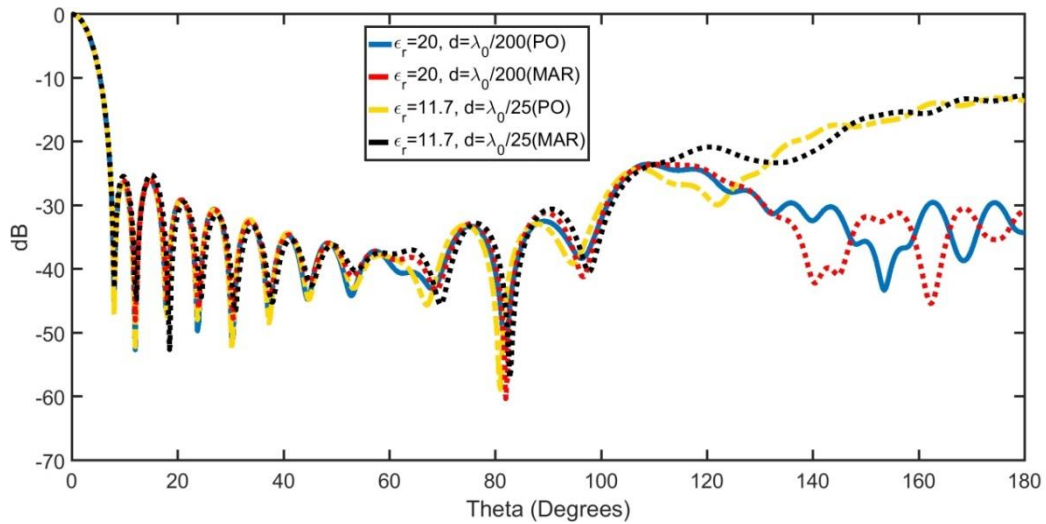


Figure 2. Total radiated fields (normalized) of the reflector in dB versus observation angle in degrees (f=5, D=10, kb=3)

If we wish to observe the effect of the dielectric coating for various parameters, we can refer to Figure 3. In this figure, the total radiated fields are plotted for several cases with different dielectric and coating thickness values.

The problem parameters are chosen as follows: the focal length (f) is 5 or 7, the aperture width (D) is 10, the width of the complex source point (kb) is 5 or 7, and the dielectric thickness (d) is  $\lambda_0/50$  or  $\lambda_0/25$ .

As depicted in Figure 3, the back radiation levels of the coated cases (PEC coated with silicon and PEC coated with tantalum oxide) are different from each other. This difference is because the impedances of the surface with these coatings, kb values and focal lengths are different. As expected, choosing thin and higher permittivity coating reduces radiation at the backside of the reflector

antenna. MAR results are also plotted to prove the correctness of PO results. Small deviations occurred at the backside as expected. Front side sidelobes are nearly same for PO and MAR.

These results provide valuable insights into the impact of dielectric coatings on the antenna's radiation pattern, particularly with regard to tune backside radiation. The difference of the impedance values for the two coatings may indicate that, under the specified parameters, the choice of either silicon or tantalum oxide as the dielectric material will yield different back radiation reduction effects. Further analysis and parameter exploration may help in understanding the nuances and optimizing the performance of the reflector antenna for specific applications.

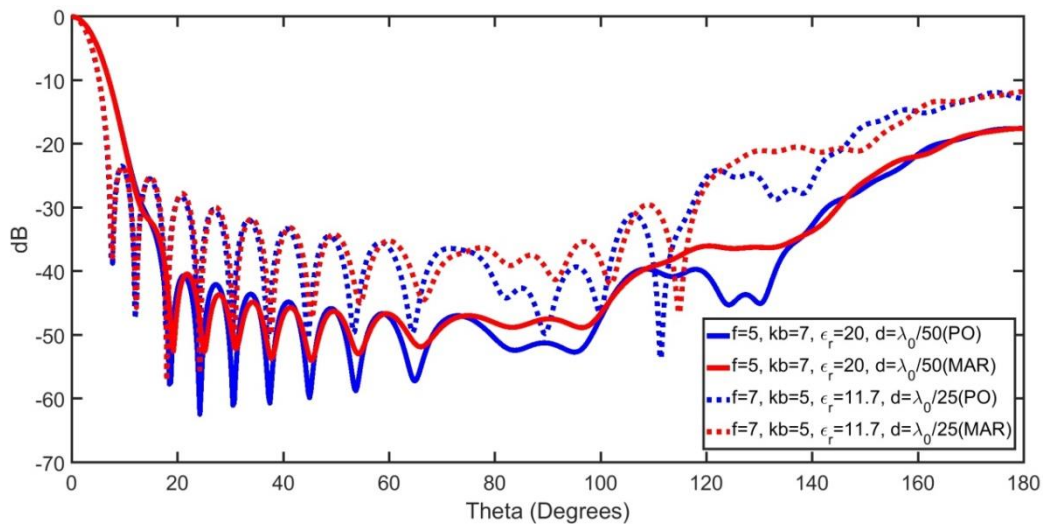


Figure 3. Total radiated fields (normalized) of the reflector in dB versus observation angle in degrees

After obtaining the directivity of the antenna using the radiation pattern distribution, the aperture efficiency is

calculated as described in equation (4). In this context, the antenna is coated with tantalum oxide, with a relative

permittivity of  $\epsilon_r=20$ . The antenna aperture width is  $D=10$ , and the thickness of the coating is chosen as  $1/100$  of the wavelength ( $d=\lambda_0/100$ ).

The analysis explores how changing the focus of the reflector affects the aperture efficiency, and the results are presented in Figure 4. Three different values of focal length ( $f$ ) are considered:  $f=3$ ,  $f=5$ , and  $f=7$ .

When  $f=3$ , the aperture efficiency slowly increases and reaches its maximum value around  $kb=1$ , then it starts to decline as  $kb$  increases. On the other hand, when  $f=5$ , the antenna exhibits low aperture efficiencies at low  $kb$  values, but the maximum aperture efficiency is higher

than that of  $f=3$ , occurring around  $kb=2$ . The highest aperture efficiency is obtained when  $f=7$ , and it gradually increases up to  $kb=5$ .

These results indicate that the focal length of the reflector significantly impacts the aperture efficiency of the antenna. Different focal lengths lead to distinct patterns of aperture efficiency variation with respect to  $kb$ . The focal length of  $f=7$  yields the highest overall aperture efficiency, while different focal lengths may exhibit varying trends in aperture efficiency behavior as a function of  $kb$ .

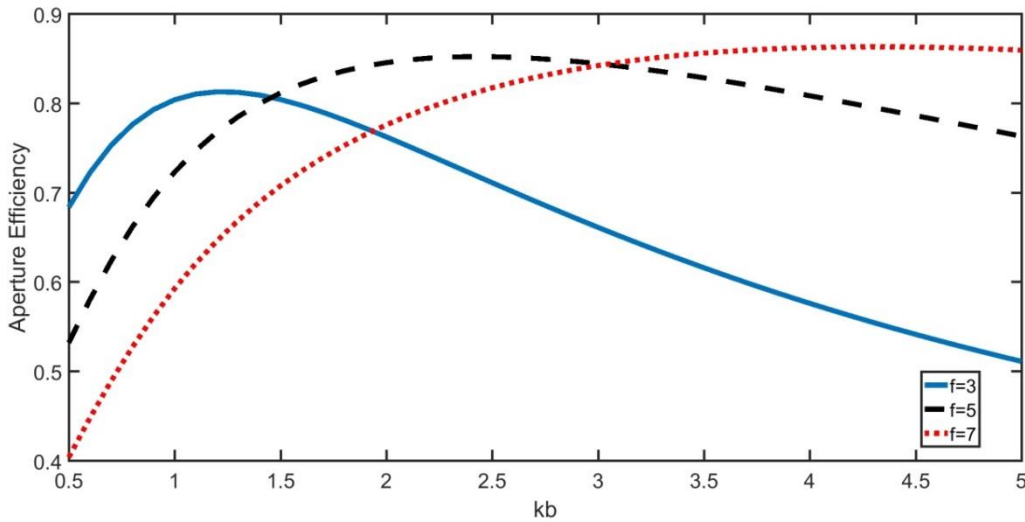


Figure 4. Aperture efficiency versus CSP width ( $kb$ ) ( $D=10$ ,  $\epsilon_r=20$ ,  $h=\lambda_0/100$ )

We present the variation of aperture efficiency versus focal distance for several CSP widths ( $kb$ ) in Figure 5. Problem parameters are  $D=10$ ,  $d=\lambda_0/100$  and  $\epsilon_r=20$ . Based on the results, we can observe that for all  $kb$  cases, the aperture efficiencies are low when the focal distance is  $f=1$ . As the focal distance increases, the aperture efficiency gradually improves, reaching its maximum value at certain focal distances, and then it starts to decrease.

This trend indicates that the focal distance plays a critical role in determining the antenna's aperture efficiency. For focal distances less than the optimum value, the antenna performance suffers, resulting in lower aperture efficiencies. However, as the focal distance increases beyond the optimum, the antenna's performance also degrades, leading to decreased aperture efficiency.

It is essential to identify the optimal focal distance for a specific CSP width ( $kb$ ) to achieve the highest aperture efficiency for the reflector antenna. Understanding these trends enables antenna designers to make informed

decisions in selecting the appropriate focal distance, ensuring optimal performance for their intended applications.

To examine the influence of relative permittivity on directivity and aperture efficiency, Figures 6(a) and 6(b) are instructive. In Figure 6(a) and (b), variations in directivity and aperture efficiency are presented for different thicknesses concerning the relative dielectric constant of the coating material.

It's evident from these figures that higher thickness values result in lower directivity and aperture efficiencies. Conversely, reducing the coating thickness leads to higher directivities and enhanced aperture efficiencies. Furthermore, it can be noted that as the relative dielectric constant of the material increases, there is a significant decrease in directivity and aperture efficiency, particularly when the thickness is high. However, the effect of dielectric constant on directivity is relatively small when the thickness is low.

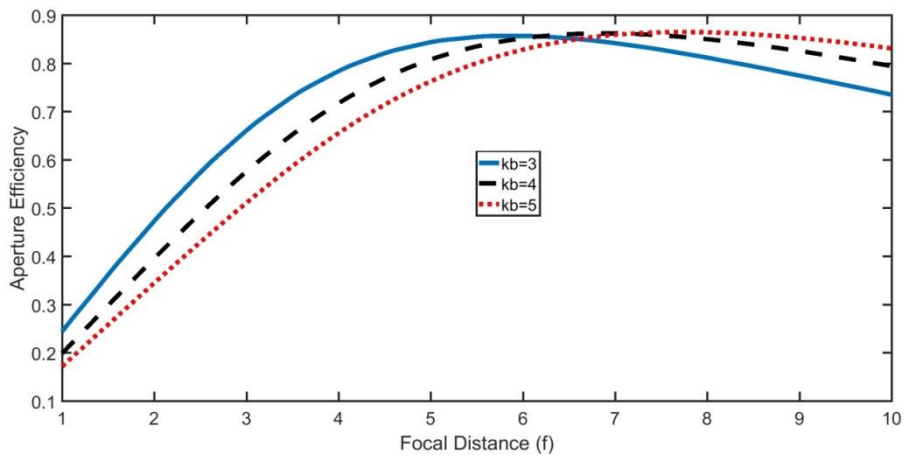


Figure 5. Aperture efficiency versus focal distance (f) ( $D=10$ ,  $\epsilon_r=20$ ,  $h=\lambda_0/100$ )

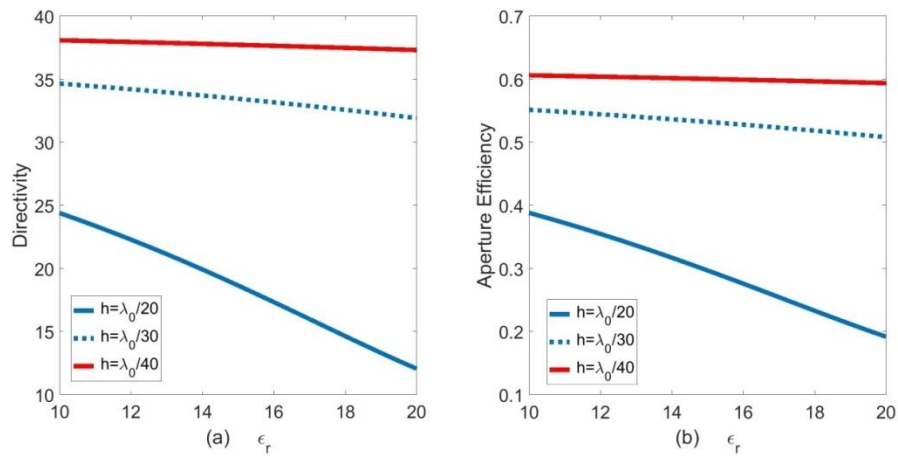


Figure 6. Directivity and aperture efficiency versus relative dielectric constant ( $D=10$ ,  $f=3$ ,  $kb=3$ )

In the final analysis, the impact of coating thickness is assessed for various dielectric constants, focal distances, and CSP width values, as illustrated in Figures 7(a) and (b). It is evident from these figures that the dielectric constant's effect on the coating becomes more dominant when the thickness is high. Reducing the thickness results in nearly identical directivity and aperture efficiency values for two different dielectric coatings. The highest directivities and aperture efficiencies are achieved when the focal distance (f) is set to 5 and the

CSP width (kb) is 3, using a specific thickness. Decreasing the focal distance (f) while keeping kb constant leads to the expected results of reduced directivity and aperture efficiencies.

In summary, these observations highlight the interplay between coating thickness, dielectric constant, focal distance, and CSP width in determining the performance of the system, with certain configurations yielding higher directivity and aperture efficiency values.

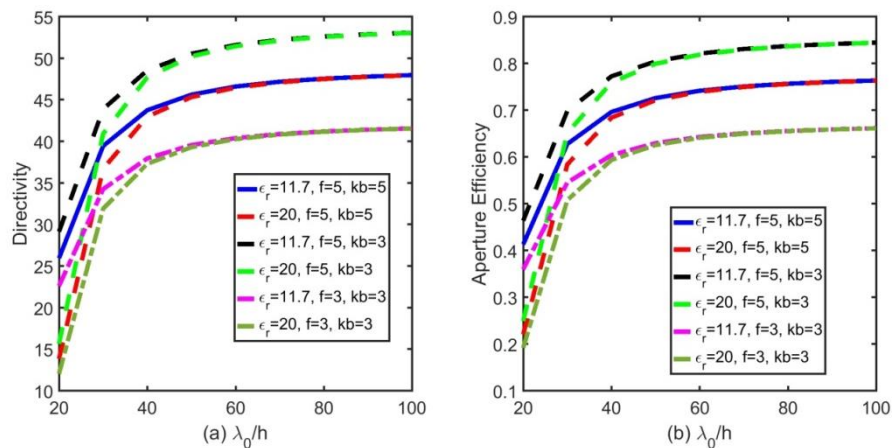


Figure 7. Directivity and aperture efficiency versus thickness of coating

**4. Conclusion**

The numerical investigation of a parabolic, cylindrical, dielectric-coated PEC reflector antenna's radiation performance yielded promising results. The study utilized the physical optics method to calculate radiated fields, total fields, and antenna efficiency parameters. The results demonstrated high aperture efficiency and tunable backside radiation levels achievable by changing the coating material on the reflector.

One notable advantage of the study was the use of the PO method, which allowed for obtaining fast and accurate results in a significantly reduced computing time. This efficiency in computation is crucial in antenna design and analysis, as it enables researchers and engineers to explore various scenarios and optimize antenna performance effectively.

The findings from this investigation can be leveraged in future studies to analyze the effects of different coatings on antenna performance. The ability to control backside radiation levels by varying the dielectric coating opens up possibilities for tailoring the antenna characteristics to suit specific applications.

In conclusion, the research presented in this study provides valuable insights into the radiation behavior of dielectric-coated PEC reflector antennas. The use of the physical optics method contributes to faster and accurate simulations, making it a powerful tool for future antenna design and analysis studies involving coatings and other parameters.

**Author Contributions**

The percentage of the author contributions is presented below. The author reviewed and approved the final version of the manuscript.

	F.K.
C	100
D	100
S	100
DCP	100
DAI	100
L	100
W	100
CR	100
SR	100
PM	100
FA	100

C=Concept, D= design, S= supervision, DCP= data collection and/or processing, DAI= data analysis and/or interpretation, L= literature search, W= writing, CR= critical review, SR= submission and revision, PM= project management, FA= funding acquisition.

**Conflict of Interest**

The author declared that there is no conflict of interest.

**Ethical Consideration**

Ethics committee approval was not required for this study because of there was no study on animals or humans. The authors confirm that the ethical policies of the journal, as noted on the journal's author guidelines page, have been adhered to.

**References**

Balanis CA. 2016. Antenna theory: analysis and design. John Wiley Sons, New Jersey, USA, 4<sup>th</sup> ed., pp: 875–920.

Bhattacharyya AK. 1995. High-frequency electromagnetic techniques: recent advances and applications. Wiley-Interscience, New York USA, pp: 487.

Bie M, Peng M, Jiang ZH, Werner DH. 2023. Modal expansion analysis inverse-design and experimental verification of a broadband high-aperture efficiency circular short backfire antenna loaded with anisotropic impedance surfaces. *IEEE Transactions Anten Propag*, 71(6): 4783-4798.

Bleszynski EH, Bleszynski MK, Jaroszewicz T. 1993. Surface-integral equations for electromagnetic scattering from impenetrable and penetrable sheets. *IEEE Antennas Propag Mag*, 35(6): 14-25.

Chang L, Chen L-L, Zhang J-Q, Chen Z-Z. 2021. A compact wideband dipole antenna with wide beamwidth. *IEEE Antennas Wirel Propag Lett*, 20(9):1701-1705.

Galuscak R, Mazanek M, Hazdra P, Kabourek V. 2018. A dual-band reflector feed in coaxial configuration for satellite communication. *IEEE Antennas Propag Mag*, 60: 89–94.

Ge L, Gao S, Zhang D, Li M. 2018. Magnetolectric dipole antenna with low profile. *IEEE Antennas Wirel Propag Lett*, 17(10): 1760-1763.

Granet C, Zhang HZ, Forsyth AR, Graves GR, Doherty P, Greene KJ, James GL, Sykes P, Bird TS, Sinclair MW, Moorey G, Manchester RN. 2005. The designing manufacturing and testing of a dual-band feed system for the Parkes radio telescopes. *IEEE Antennas Propag Mag*, 47: 13–19.

Kuyucuoglu F, Oğuzer T, Avgin I, Altintas A. 2014. Analysis of an arbitrary-profile cylindrical impedance reflector surface illuminated by an E-polarized complex line source beam. *J Electromag Waves Applicati*, 28(3): 360-377.

Lu S, Qu SW. 2023. Low-profile dual-band reflector antenna for high-frequency applications. *Sensors*, 23(13): 5781.

Maliuzhinets G. D. 1959. Excitation reflection and emission of surface waves from a wedge with given face impedance. *Sov Phys Dokl*, 3: 752–755.

Qudrat-E-Maula M, Shafai L. 2012. Low-cost microstrip-fed printed dipole for prime focus reflector feed. *IEEE Trans Antennas Propag*, 60(11): 5428-5433.

Rahmat-Samii Y, Haupt R. 2015. Reflector antenna developments: A perspective on the past present and future. *IEEE Antennas Propag Mag*, 57 (2): 85–95.

Tiberio R, Pelosi G, Manara G. 1985. A uniform GTD formulation for the diffraction by a wedge with impedance faces. *IEEE Trans Antennas Propag*, 33: 867–873.

Umul YZ. 2006. Modified theory of the physical-optics approach to the impedance wedge problem. *Opt Lett*, 31: 401–403.

Umul YZ. 2007. Edge-dislocation waves in the diffraction process by an impedance half-plane. *J Opt Soc Am A*, 24: 507–511.

Umul YZ. 2008. Scattering of a line source by a cylindrical parabolic impedance surface. *JOSA A* 25(7): 1652-1659.

Volakis JL. 1986. A uniform geometrical theory of diffraction for an imperfectly conducting half-plane *IEEE Trans. Antennas Propag*, 34: 172–180.



- Wang C, Wu J, Ma B-Y, Guo Y-X. 2020. A 3D-printed K/Ka-band dual circularly polarized feed for offset-fed reflector antennas. In: Proceedings of the IEEE Asia-Pacific Microwave Conference, December 8–11, Hong Kong, China, pp. 558–560.
- Wu L, Peng S, Xu J, Xiao Z. 2016. A W-band radiometer with the offset parabolic antenna for radiometric measurements. *Int J Antennas Propag*, 2016: 1–9.
- Wu R, Xue Q, Chu QX, Chen FC. 2021. Ultrawideband dual-polarized antenna for LTE600/LTE700/GSM850/GSM900 application. *IEEE Antennas Wirel Propag Lett*, 20(7): 1135–1139.